Article

Low-Temperature Rapid-Scan Detection of Reactive Intermediates in Epoxidation Reactions Catalyzed by a New Enzyme Mimic of Cytochrome P450

Natalya Hessenauer-Ilicheva, Alicja Franke, Dominik Meyer, Wolf-D. Woggon, and Rudi van Eldik

J. Am. Chem. Soc., **2007**, 129 (41), 12473-12479• DOI: 10.1021/ja073266f • Publication Date (Web): 19 September 2007

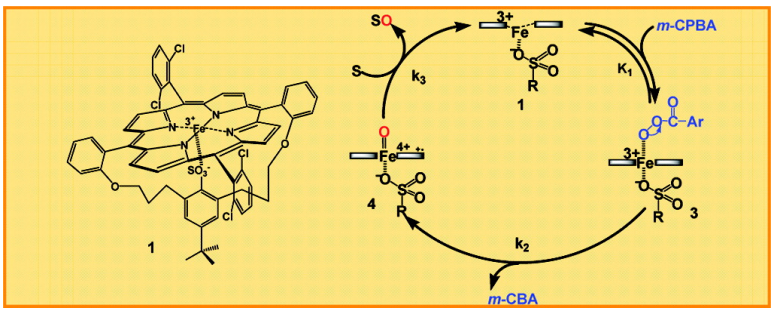

More About This Article

Additional resources and features associated with this article are available within the HTML version:

- Supporting Information
- Links to the 8 articles that cite this article, as of the time of this article download
- Access to high resolution figures
- Links to articles and content related to this article
- Copyright permission to reproduce figures and/or text from this article

View the Full Text HTML

J|A|C|S
ARTICLES
Published on Web 09/19/2007

Low-Temperature Rapid-Scan Detection of Reactive Intermediates in Epoxidation Reactions Catalyzed by a New Enzyme Mimic of Cytochrome P450

Natalya Hessenauer-Ilicheva,[†] Alicja Franke,[†] Dominik Meyer,[‡] Wolf-D. Woggon,*[,‡] and Rudi van Eldik*[,†]

Contribution from the Institute for Inorganic Chemistry, University of Erlangen-Nürnberg, Egerlandstrasse 1, 91058 Erlangen, Germany, and Department of Chemistry, University of Basel, St. Johanns-Ring 19, 4056 Basel, Switzerland

Received May 8, 2007; E-mail: vaneldik@chemie.uni-erlangen.de

Abstract: The use of synthetic iron(III) porphyrins as models for heme-type catalysts in biomimetic cytochrome P450 research has provided valuable information on the nature and reactivity of intermediates produced in the "peroxide shunt" pathway. This article reports spectroscopic detection of reactive intermediates formed in the epoxidation reaction of *cis*-stilbene with *m*-chloroperoxybenzoic acid catalyzed by a new mimic of cytochrome P450 with a substituted RSO_3^- group (**1**). The application of low-temperature rapid-scan stopped-flow techniques enabled the determination of equilibrium and rate constants for the formation and decay of all intermediates in the catalytic cycle of **1**, including the rate constant for the formation (**1**$^{\bullet+}$)Fe^{IV}=O and for oxygen transfer to the substrate. Noteworthy, the reaction of (**1**$^{\bullet+}$)Fe^{IV}=O with *cis*-stilbene leads to an almost complete re-formation (95%) of the starting complex **1**. The results show that complex **1** is a valuable catalyst with promising properties for further applications in a biomimetic approach toward mimicking oxygenation reactions of cytochrome P450.

Introduction

Elucidation of the mechanism of reactive intermediate formation in oxygenation reactions catalyzed by cytochrome P450 enzymes is essential to understand the chemistry of in vivo processes and is of continued interest in biological and bioinorganic chemistry. Therefore, over the past three decades biomimetic approaches toward mimicking the oxygenation reactions of these enzymes have focused on synthetic iron(III) porphyrin complexes and their interaction with oxygen donors such as iodosylbenzene, peroxy acids, and hydroperoxides.[1] It was clearly demonstrated that the nature and reactivity of the intermediates produced via a "peroxide shunt" pathway can easily be tuned by (1) the electronic and steric properties of the porphyrin moiety, (2) variation of the central metal atom or axial ligands, (3) changing the reaction conditions (i.e., pH, protic vs aprotic solvent, temperature), and (4) the chemical nature of the oxidant used. Although it has been generally implicated in the literature that an oxo−iron(IV) porphyrin cation radical ((Por$^{\bullet+}$)Fe^{IV}=O, referred to as compound I = CpdI in the catalytic cycle of heme-containing enzymes) is formed as a reactive intermediate in the reactions of iron(III) porphyrin complexes with oxidants,[1,2] direct characterization of (Por$^{\bullet+}$)Fe^{IV}=O species has been very difficult because of their high reactivity in subsequent reactions.

Recently, Woggon et al. synthesized two new enzyme mimics for cytochrome P450 in which the RS^- ligand is replaced by an RSO_3^- group (complexes **1** and **2** in Figure 1).[3] Substitution of the S^- donor in P450 by an RSO_3^- group in these complexes significantly reduces the negative charge density on the fifth axial ligand and remarkably tunes the redox potential of Fe$^{III/II}$ to that measured for the resting state of $P450_{cam}$.[3b] Moreover, although coordination by the thiolate ligand was changed to the RSO_3^- group, complexes **1** and **2** were shown to be valuable P450 models with respect to electrochemistry and displayed a good reactivity toward alkene epoxidation (with a turnover

[†] University of Erlangen-Nürnberg.
[‡] University of Basel.

(1) (a) McLain, J. L.; Lee, J. J.; Groves, T. In *Biomimetic Oxidations Catalyzed by Transition Metal Complexes;* Meunier, B., Ed.; Imperial College Press: London, 2000; pp 91−169. (b) Meunier, B. In *Metalloporphyrins Catalyzed Oxidations;* Montanari, F., Casella, L., Eds.; Kluwer Academic Publishers: Dordrecht, The Netherlands, 1994; pp 1−47. (c) Shimada, H.; Sligar, S. G.; Yeom, H.; Ishimura, Y. In *Oxygenases and Model Systems;* Funabiki, T., Ed.; Kluwer Academic Publishers: Dordrecht, The Netherlands, 1997; pp 195−221. (d) Watanabe, Y. In *Oxygenases and Model Systems;* Funabiki, T., Ed.; Kluwer Academic Publishers: Dordrecht, The Netherlands, 1997; pp 223−282. (e) Traylor, T. G.; Traylor, P. S. In *Active Oxygen in Biochemistry;* Valentine, J. S., Foote, C. S., Greenberg, A., Liebman, J. F., Eds.; Chapman & Hall: London, 1995; pp 84−187.

(2) (a) Nam, W.; Park, S.-E.; Lim, I. K.; Lim, M. H.; Hong, J.; Kim, J. *J. Am. Chem. Soc.* **2003**, *125*, 14674. (b) Goh, Y. M.; Nam, W. *Inorg. Chem.* **1999**, *38*, 914. (c) Groves, J. T.; Haushalter, R. C.; Nakamura, M.; Nemo, T. E.; Evans, B. J. *J. Am. Chem. Soc.* **1981**, *103*, 2884. (d) Groves, J. T.; Watanabe, Y. *J. Am. Chem. Soc.* **1988**, *110*, 8443. (e) Gross, Z.; Nimri, S. *Inorg. Chem.* **1994**, *33*, 1731.

(3) (a) Woggon, W.-D.; Leifels, T.; Sbaragli, L. *Cytochromes P450: Biochemistry, Biophysics and Drug Metabolism*, 13th International Conference on Cytochromes P450, Prague, Czech Republic, June 29−July 3, 2003. (b) Meyer, D.; Woggon, W.-D. *Chimia* **2005**, *59*, 85. (c) Woggon, W.-D. *Acc. Chem. Res.* **2005**, *38*, 127. (d) Kozuch, S.; Leifels, T.; Meyer, D.; Sbaragli, L.; Shaik, S.; Woggon, W.-D. *Synlett* **2005**, *4*, 675. (e) Sbaragli, L.; Woggon, W.-D. *Synthesis* **2005**, *9*, 1538. (f) Meyer, D.; Leifels, T.; Sbaragli, L.; Woggon, W.-D. *Biochem. Biophys. Res. Commun.* **2005**, *338*, 372.

10.1021/ja073266f CCC: $37.00

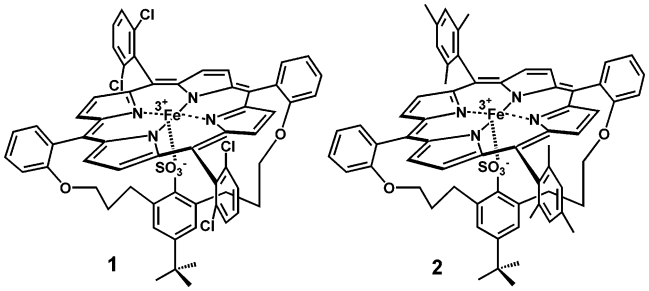

Figure 1. RSO_3^--substituted new enzyme mimics of cytochrome P450 (complexes **1** and **2**).

number up to 1800 for **1**), hydrocarbon hydroxylation, N-dealkylation, and diol cleavage.[3e,f]

Herein, we report spectroscopic and kinetic information on the formation of the reactive iron(IV)−oxo porphyrin radical cation ((**1**$^{\bullet+}$)Fe^{IV}=O) during the reaction of complex **1** with *m*-chloroperoxybenzoic acid (*m*-CPBA) in acetonitrile and direct measurement of the rate constants for the epoxidation of *cis*-stilbene by the CpdI analogue. The use of low-temperature, rapid-scan, stopped-flow techniques revealed the complete UV−vis spectral changes related to the formation and decay of the intermediates involved in the oxygen activation cycle catalyzed by complex **1**.

Experimental Section

Materials. All solutions were prepared in acetonitrile (99.9% AMD CHROMASOLV from Sigma-Aldrich). Complexes **1** and **2** were prepared as described in the literature and characterized by X-ray, UV−vis, EPR, and ESI-MS spectroscopy.[3] *cis*-Stilbene (96%) was purchased from Aldrich. *m*-Chloroperoxybenzoic acid was purchased from Acros Organics and purified before use by recrystallization from hexane.

GC-FID Experiments. A solution of **1** (4.8 mL) in CH_3CN was cooled to −35 °C (acetone/dry ice bath) in a dry 10-mL two-necked flask containing a stir bar and a low temperature thermometer. An *m*-CPBA solution (0.1 mL) in CH_3CN was added and reacted with the former for at least 0.5 min (changes in optical properties of the reaction solution from brownish to green were observed during this period). After that, 3.5 μL of *cis*-stilbene was added, and samples (∼1.5 mL) were taken after an additional 1.5, 5, and 20 min. The latter were filtered through basic alox to remove *m*-CPBA, partially concentrated at reduced pressure, and injected into GC-FID for analysis. GC analysis was performed on a Thermo Finnigan Focus GC-FID with a 15-m Supelcowax SE-54 column (i.d. 0.25 mm). Product peaks were confirmed by co-injection of the corresponding commercially available substance. The concentrations of the solutions were chosen such that in the final reaction mixture the concentrations were [*m*-CPBA] = 1.6×10^{-4} M, [*cis*-stilbene] = 4×10^{-3} M, and [**1**] = 8.6×10^{-6} M.

Additional experiments were performed under similar conditions, where upon *cis*-stilbene addition, the complete reaction was quickly brought to room temperature after 5 min and filtered over basic alox, concentrated at reduced pressure, and injected into the GC-FID. Yields were calculated from the addition of known quantities of *cis*-stilbene. Control experiments were performed by cooling 4.9 mL of a solution of *m*-CPBA in CH_3CN to −35 °C (acetone/dry ice bath) in a dry 10-mL two-necked flask containing a stir bar and a low temperature thermometer. *cis*-Stilbene (3.5 μL) was added, and other samples (∼1.5 mL) were taken after 1.5, 5, and 20 min, or the complete reaction volume was brought to room temperature quickly 5 min after addition of *cis*-stilbene. The so-obtained samples were filtered through basic alox to remove *m*-CPBA, partially concentrated at reduced pressure, and injected into the GC-FID for analysis. The concentrations were chosen to be the same as those in the former experiments.

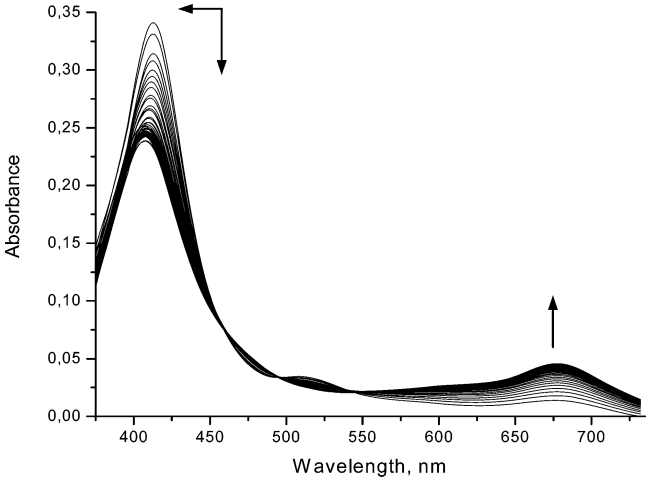

Figure 2. Rapid-scan spectra recorded for the formation of (**1**$^{\bullet+}$)Fe^{IV}=O in the reaction of **1** with *m*-CPBA. Experimental conditions: [**1**] = 4.3×10^{-6} M, [*m*-CPBA] = 5.4×10^{-5} M in acetonitrile at −35 °C.

Low-Temperature Stopped-Flow Instrument and Software. Time-resolved UV−vis spectra were recorded with a Hi-Tech SF-3L low-temperature stopped-flow unit (Hi-Tech Scientific) equipped with a J&M TIDAS 16/300-1100 diode array spectrophotometer (J&M). The optical cell had a light path of 1.0 cm and was connected to the spectrophotometer unit with flexible light guides. Five-milliliter driving syringes were used. The mixing chamber was immersed in an ethanol bath that was placed in a Dewar flask containing liquid nitrogen. The ethanol bath was cooled by liquid nitrogen evaporation, and its temperature was measured by use of a Pt resistance thermometer and maintained at ±0.1 °C by use of a PID temperature-controlled thyristor heating unit (both Hi-Tech). Complete spectra were collected between 370 and 770 nm with the integrated J&M software Kinspec 2.30.

Low-Temperature Spectral Measurements. Time-resolved UV−vis spectra were recorded with a quartz glass dip-in detector (Spectralytics) coupled to a J&M TIDAS 16/300-1100 diode array spectrophotometer (J&M). The optical dip-in detector had a light path of 1.0 cm and was connected to the spectrophotometer unit with flexible light guides. A 20-mL double wall reaction vessel was used and thermostated (±0.1 °C) by a combination of cold methanol circulation (Colora WK 14-1 DS) and an 800 W heating unit. Complete spectra were recorded between 370 and 770 nm with the integrated J&M software Kinspec 2.30.

Kinetic Simulations. Simulations were performed with the use of Specfit, Global Analysis System, version 3.0.38 for 32-bit Windows system.

Results and Discussion

Rapid stopped-flow mixing of **1** with an excess of *m*-CPBA in acetonitrile at −35 °C led to spectral changes characterized by a much weaker Soret band at 409 nm and broad absorption bands around 575−750 nm, characteristic of a (Por$^{\bullet+}$)Fe^{IV}=O species[2d] (Figure 2).

Kinetics of the formation of **1**$^{\bullet+}$(Fe^{IV})=O was studied under pseudo-first-order conditions (i.e., $10 \le$ [*m*-CPBA]/[**1**] ≤ 200) in acetonitrile at −35 °C. k_{obs} values obtained from a single-exponential fit to the absorbance-time traces showed clear saturation at high oxidant concentrations ([*m*-CPBA]/[**1**] > 100; Figure 3). These results suggest a two-step process passing through the acylperoxo−iron(III) porphyrin intermediate **3**, which subsequently forms **4** (CpdI) by O−O bond cleavage as shown in Figure 4. The formation of such acylperoxo−iron(III) porphyrin intermediates has been experimentally evidenced in the reaction of Fe^{III}(TMP)(OH) (where TMP = tetramesityl

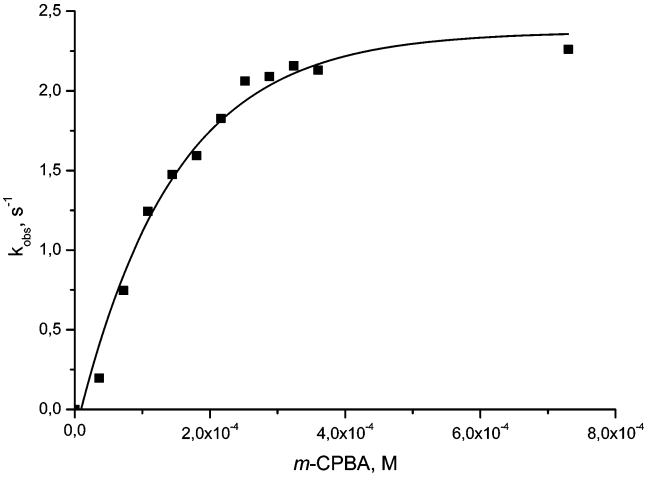

Figure 3. *m*-CPBA concentration dependence of k_{obs}. Experimental conditions: [**1**] = 3.6 × 10^{-6} M, [*m*-CPBA] = (0.36−7.2) × 10^{-4} M in acetonitrile at −35 °C.

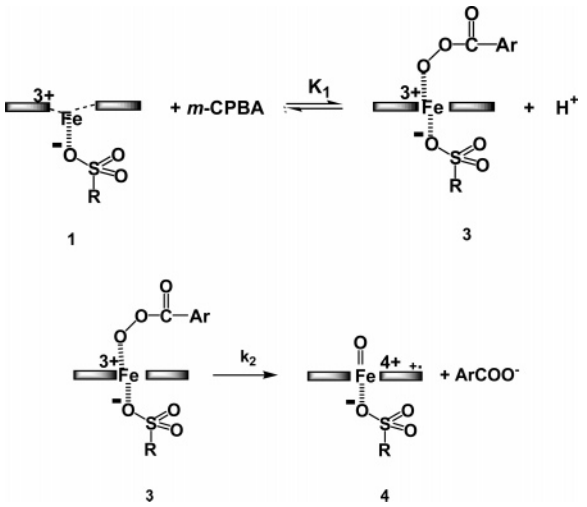

Figure 4. Reaction sequence deduced from the *m*-CPBA concentration dependence of k_{obs} (Figure 3).

iron porphyrin) with *m*-CPBA[2d] as well as in a very recent study by Nocera et al.[4] dealing with *m*-CPBA oxidation reactions of ferric Hangman porphyrin complexes possessing acid−base functional groups over the face of the redox-active macrocycles. Noteworthy, all these findings correspond to earlier experiments with polyethylene-glycolated HRP in which saturation kinetics could be observed only in apolar non-protic media.[5] However, accumulation of the acylperoxo−iron(III) porphyrin **3** was not observed under the employed reaction conditions in the present study.

In contrast, the kinetics of the reaction between complex **2** and *m*-CPBA under identical conditions results in an almost linear dependence of k_{obs} on [*m*-CPBA] with only slight saturation at very high oxidant concentration (>1.2 mM).[6] The distinct behavior of **1** and **2** can be attributed to the difference in electron donation ability of the porphyrin ligand, which is known to trigger the rate of O−O bond cleavage,[7−9] such that electron-deficient porphyrins can achieve saturation kinetics in the reactions with oxidants "earlier" than their electron-rich analogues.

Saturation kinetics for the formation of **4** enabled us to determine separately the value of the pre-equilibrium constant, K_1, ascribed to the reversible formation of **3** (Figure 4) and the value of the first-order constant, k_2, ascribed to O−O bond cleavage in the acylperoxo−iron(III) porphyrin intermediate **3**.

$$k_{obs} = \frac{k_2 K_1 [m\text{-CPBA}]}{1 + K_1 [m\text{-CPBA}]}$$

At low oxidant concentration, $1 \gg K_1[m\text{-CPBA}]$ and $k_{obs} = k_2K_1[m\text{-CPBA}]$, whereas at high [*m*-CPBA], k_{obs} becomes independent of the oxidant concentration and equals k_2. The values of K_1 and k_2 determined from the data presented in Figure 3 are (4.4 ± 0.5) × 10^3 M^{-1} and 2.4 ± 0.1 s^{-1} at −35 °C, respectively. The first-order rate constant, k_2, for heterolytic cleavage of the O−O bond in intermediate **3** is significantly higher than that reported by Ozaki et al.[5] for the reaction of polyethylene-glycolated HRP with hydrogen peroxide in chlorobenzene (viz. 1.0 s^{-1} at 7.5 °C) and that determined by Groves and Watanabe[2d] for the reaction between Fe^{III}TMP(OH) and *m*-CPBA in dichloromethane (viz. 0.01 s^{-1} at −34 °C). However, because of the very different reaction conditions employed in our and the above-mentioned studies, especially the polarity of the solvents used (more polar CH_3CN should stabilize more the products from heterolytic O−O bond cleavage), chemical nature of the oxidants and catalyst, and the different electron-donating and -withdrawing properties of the porphyrin rings, it is difficult to evaluate the real effect of the RSO_3^- group in complex **1** on the rate of O−O bond cleavage in **3**. On the other hand, an ongoing investigation[10] of the oxidation reaction of a thiolate-substituted iron(III) porphyrin model (**SR** complex[11]) with *m*-CPBA as oxidant in acetonitrile at −35 °C revealed that the second-order rate constant for the formation of the (Por$^{\bullet+}$)Fe^{IV}=O intermediate with RS$^-$ as proximal ligand is almost 4 times lower than that found in the present study for complex **1** under similar reaction conditions. Since it can be expected that a stronger donor ligand such as the RS$^-$ group should increase the rate of O−O bond cleavage (homolytic or heterolytic), the observed lower reactivity of the **SR** complex toward oxidation is probably due to a less efficient equilibration for the formation of the acylperoxo−iron(III) porphyrin intermediate (the *trans* effect from the sulfur of thiolate proximal ligand could be responsible for such behavior). However, more detailed mechanistic studies on the oxidation reaction of the **SR** complex are required to account for the observed differences in the reactivity of iron(III) porphyrin models with RSO_3^- and RS$^-$ proximal ligands.

With regard to the electronic effect of the axial ligands on the mode of O−O bond cleavage in acylperoxo−iron(III) porphyrins,[12] it is supposed that a stronger electron-donating axial ligand will enhance heterolytic O−O bond scission.

(4) Soper, J. D.; Kryatov, S. V.; Rybak-Akimova, E. V.; Nocera, D. G. *J. Am. Chem. Soc*. **2007**, *129*, 5069.
(5) Ozaki, S.-i.; Inada, Y.; Watanabe, Y. *J. Am. Chem. Soc.* **1998**, *120*, 8020.
(6) Hessenauer-Ilicheva, N.; Franke, A.; Meyer, D.; Woggon, W.-D.; van Eldik, R. University of Erlangen-Nürnberg, Germany, and University of Basel, Switzerland. Work in progress, 2007.
(7) Groves, J. T.; Watanabe, Y. *Inorg. Chem.* **1987**, *26*, 785.
(8) Yamaguchi, K.; Watanabe, Y.; Morishima, I. *J. Am. Chem. Soc.* **1993**, *115*, 4058.
(9) Nam, W.; Choi, S. K.; Lim, M. H.; Rohde, J.-U.; Kim, I.; Kim, J.; Kim, C.; Que, L., Jr. *Angew. Chem., Int. Ed.* **2003**, *42*, 109.
(10) Work in progress.
(11) Higuchi, T.; Uzu, S.; Hirobe, M. *J. Am. Chem. Soc*. **1990**, *112*, 7051.
(12) (a) Franzen, S.; Roach, M. P.; Chen, Y.-P.; Dyer, R. B.; Woodruff, W. H.; Dawson, J. H. *J. Am. Chem. Soc.* **1998**, *120*, 4658. (b) Higuchi, T.; Shimada, K.; Maruyama, N.; Hirobe, M. *J. Am. Chem. Soc*. **1993**, *115*, 7551.

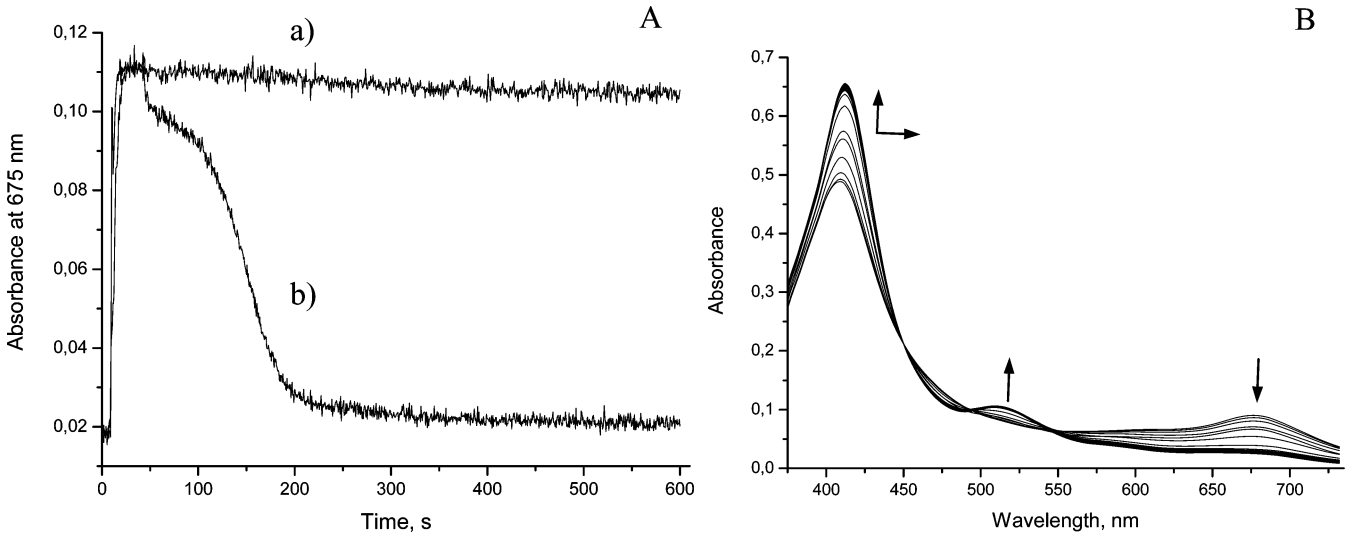

Figure 5. (A) Kinetic traces recorded with the dip-in detector at 675 nm for the formation and decay of **4**. (a) In the absence of the substrate. (b) After addition of 2.07×10^{-3} M *cis*-stilbene to the solution of **4**. Experimental conditions: [**1**] = 8.4×10^{-6} M, [*m*-CPBA] = 8.4×10^{-5} M in acetonitrile at −35 °C. (B) Spectral changes recorded during re-formation of the starting complex **1** in the presence of the substrate. Experimental conditions: [**1**] = 7.9×10^{-6} M, [*m*-CPBA] = 7.9×10^{-5} M, [*cis*-stilbene] = 1.6×10^{-2} M in acetonitrile at −35 °C.

However, the latest findings by Nam et al.[13] suggest that the electron density on the O−O bond must be optimized for heterolytic cleavage (i.e., it should not be too small but also not too large). They have demonstrated that axial ligands with weaker electron donors (i.e., $CF_3SO_3^-$, ClO_4^-, NO_3^-) favor heterolytic O−O bond scission to form $(Por^{\bullet+})Fe^{IV}{=}O$ species, whereas iron(III) porphyrin complexes with stronger donor ligands prefer homolytic O−O bond cleavage to produce iron(IV) porphyrin complexes or iron(III) porphyrin *N*-oxides. In the present study, we used *m*-CPBA as oxidant, which is known to facilitate heterolytic O−O bond scission (due to the strong electron-withdrawing properties of its acyl group), such that on the basis of the mentioned findings it is reasonable to expect that the RSO_3^- ligand and electron-deficient porphyrin ring in complex **1** should favor heterolytic O−O bond cleavage of the acylperoxo−iron(III) porphyrin intermediate in comparison to other model iron(III) porphyrin complexes that possess a strong donating axial and/or porphyrin ligands.

In the absence of reactive substrates, the oxo−iron porphyrin radical cation **4** is stable for almost 600 s at −35 °C and [*m*-CPBA] = 7.3×10^{-4} M in acetonitrile (Figure 5a). The addition of *cis*-stilbene to the green solution of **4** results in a fast decomposition of **4** with concomitant 95% regeneration of the starting complex **1** (Figure 5b).

To evaluate the effect of substrate concentration on the reaction between **4** and *cis*-stilbene, kinetic studies were performed in which the solutions of **1** (7.9×10^{-6} M) containing various amount of *cis*-stilbene (($6.3-111) \times 10^{-4}$ M) were mixed with a solution of *m*-CPBA (7.9×10^{-5} M), and the re-formation of **1** (the product of reaction between **4** and substrate) was monitored at 412 nm in acetonitrile at −35 °C. The reaction profile is characterized by a rapid decrease in the concentration of **1** (due to formation of **4**) followed by an apparent induction period that depends on the excess of substrate employed (Figure 6). If the *cis*-stilbene concentration is kept below a 500-fold excess, **4** is always sufficiently and rapidly regenerated by the 10-fold excess of *m*-CPBA (∼20 s in the absence of *cis*-stilbene) such that the Soret band of **1** at 412 nm is not observed. This leads to a delay in the re-formation of **1** during which most of the *m*-CPBA is consumed and which can last hundreds of seconds when the excess of *cis*-stilbene is small. This observation was confirmed by experiments in which the *cis*-stilbene concentration was kept constant at 500:[**1**] and the *m*-CPBA concentration was varied from a 5- to 20-fold excess with respect to [**1**]. As can be seen from Figure 7, the apparent induction period depends strongly on the oxidant concentration and is longer for higher [*m*-CPBA].

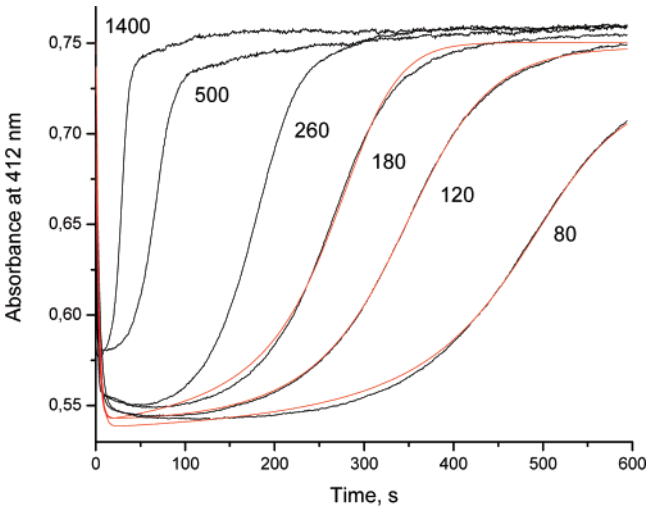

Figure 6. Typical kinetic traces recorded at 412 nm and −35 °C in acetonitrile for the reaction of **1** (7.9×10^{-6} M) with *m*-CPBA (7.9×10^{-5} M) in the presence of 6.35×10^{-4} (80), 9.53×10^{-4} (120), 1.43×10^{-3} (180), 2.06×10^{-3} (260), 3.95×10^{-3} (500), and 1.11×10^{-2} (1400) M *cis*-stilbene. The substrate excess in parentheses refers to **1**. Kinetic traces in red represent results of simulations obtained after introduction of the appropriate kinetic/thermodynamic constants and oxidant/catalyst/substrate concentrations for the reaction scheme proposed in Figure 9.

Furthermore, the occurrence of the catalytic cycle of **1** during the apparent induction period was supported by the GC-FID product analysis experiments. The epoxidation reactions of *cis*-

(13) (a) Nam, W.; Jin, S. W.; Lim, M. H.; Ryu, J. Y.; Kim, C. *Inorg. Chem.* **2002**, *41*, 3647. (b) Nam, W.; Lim, M. H.; Oh, S.-Y.; Lee, J. H.; Lee, H. J.; Woo, S. K.; Kim, C.; Shin, W. *Angew. Chem., Int. Ed.* **2000**, *39*, 3646. (c) Nam, W.; Lim, M. H.; Oh, S.-Y. *Inorg. Chem.* **2000**, *39*, 5572.

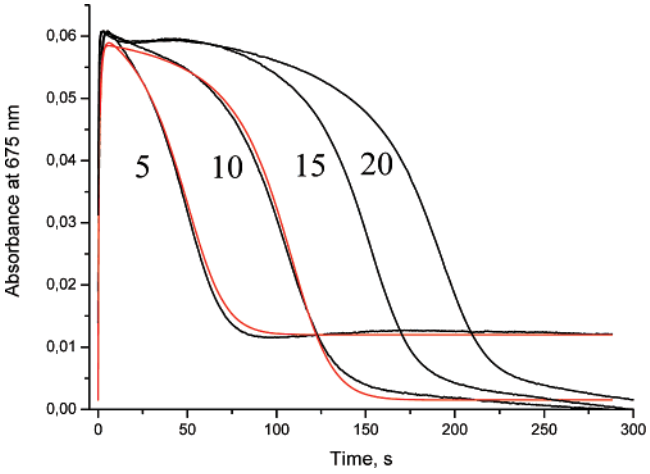

Figure 7. Typical kinetic traces recorded at 675 nm and −35 °C in acetonitrile for the reaction of **1** with 3.95×10^{-5} (5), 7.9×10^{-5} (10), 1.18×10^{-4} (15), and 1.58×10^{-4} M (20) *m*-CPBA in the presence of 3.95×10^{-3} M *cis*-stilbene. The oxidant excess in parentheses refers to the concentration of complex **1**. Kinetic traces in red represent results of simulations obtained after introduction of the appropriate kinetic/thermodynamic constants and oxidant/catalyst/substrate concentrations for the reaction scheme proposed in Figure 9.

stilbene applying complex **1** were carried out under the experimental conditions where a significant induction period was observed (i.e., [*m*-CPBA] = 1.6×10^{-4} M, [*cis*-stilbene] = 4×10^{-3} M, [**1**] = 8.6×10^{-6} M as in Figure 7), and samples were taken for GC-FID product analysis 90 s after addition of *cis*-stilbene (under the selected conditions this is well within the observed induction period). Product analysis of the so-obtained samples revealed major formation of oxidation products a−c shown in Figure 8.

Product formation further increased during the course of the reaction as concluded from further samples taken 5 min after the addition of *cis*-stilbene. For these samples, the total yield of oxidation products could be determined to be 40−50% with respect to the applied *m*-CPBA concentration in the ratio of 100/55/37 for a/b/c. Control reactions performed under similar conditions omitting **1** showed no formation of the epoxidation products even for samples taken after elongated reaction times (20 min). Epoxidation products such as a, b, and c obtained in the present study are not uncommon and have been noted in product analysis of epoxidation reactions of *cis*-stilbene catalyzed by other iron(III) porphyrins.[14] However, the product distribution of a, b, and c seems to differ slightly from that reported previously, indicating formation of significant amounts of *trans*-stilbene epoxide and a side product such as deoxybenzoin. A possible explanation for this behavior can involve the spin-state specificity of the reactive species (i.e., $\mathbf{1}^{\bullet+}(Fe^{IV})$═O). As a theoretical study revealed,[15] the different products generated in the alkene epoxidation reactions catalyzed by high-valent iron−oxo species can result from the multistate reactivity of the CpdI models, viz., the low-spin doublet states are effectively involved in the stereospecific epoxide production, whereas the high-spin quartet states lead to an increase either in the formation of epoxides that do not conserve the isomeric identity of the alkene (trans or cis) and/or in the formation of byproducts. The loss of stereochemical information during the epoxidation reaction of *cis*-stilbene catalyzed by **1** can indicate that the reactive intermediate is a two-state oxidant with predominant high-spin character under the selected reaction conditions (especially at low temperature). Indeed, this observation is in line with the reported DFT studies on the reactivity pattern of the $\mathbf{1}^{\bullet+}(Fe^{IV})$═O species.[3d]

Taken together, these results demonstrate the occurrence of a complete P450-like catalytic cycle (Figure 9) and are consistent with fast formation of the CpdI analogue **4** within ∼20 s at −35 °C and a subsequent rate-determining reaction of **4** with the substrate *cis*-stilbene. The credibility of the proposed mechanistic scheme was confirmed by simulations of the kinetic traces (Specfit) by using the thermodynamic/kinetic constants determined experimentally and the appropriate oxidant/catalyst/substrate concentration ratios. The simulated kinetic traces display a good and satisfactory agreement with the experimental traces (i.e., the observed induction periods can be nicely reproduced by introducing appropriate concentrations of *m*-CPBA and substrate into the reaction scheme proposed in Figure 9). Examples of kinetic traces simulated for different *cis*-stilbene or *m*-CPBA concentrations are shown in red in Figures 6 and 7, respectively.

Control experiments using an excess of complex **1** over **4** revealed no evidence for the formation of a Fe(IV)−oxo species as a result of a possible comproportionation reaction between **1** and **4** under the studied conditions. Furthermore, no evidence for the formation of a **4**−*cis*-stilbene intermediate was observed, although Groves and Watanabe[16] claimed formation of a $(Por^{\bullet+})Fe^{IV}$═O olefin adduct in the reaction of $TMP^{\bullet+}(Fe^{IV})$═O with cyclooctene in dichloromethane.[17]

The observed pseudo-first-order rate constants (k_{obs}^{ox}) measured for the reaction between **4** and a large excess of *cis*-stilbene (following the apparent induction period) show a linear dependence on [*cis*-stilbene] with an almost zero intercept (Figure 10). The second-order rate constant determined on the basis of these data is $k_3 = 7.0 \pm 0.2$ M^{-1} s^{-1} at −35 °C. In view of the observed induction period (Figures 6 and 7) and the available kinetic data, it can be concluded that during the induction period k_2K_1[**1**][*m*-CPBA] = k_3[**4**][*cis*-stilbene] such that the concentration of **4** not only remains constant but also represents the major iron species in solution. If typical concentrations and the above-quoted rate and equilibrium constants are substituted in this equation, it follows that [**4**] ≫ [**1**], which is in good agreement with the spectral observations and the fact that k_2K_1 is ca. 3 orders of magnitude larger than k_3.

In general, studies on the reactivity of CpdI models toward various organic substrates demonstrated that the presence and nature of the axial ligands significantly affect not only the rate of olefin oxidations but also the selectivity of the model catalysts toward substrates and the stability of the oxidants in the overall catalytic cycle.[16,18] Indeed, a Raman study[19] on the Fe−O bond strength in the series of various X-substituted $(TMP^{\bullet+})Fe^{IV}$(O)(X) derivatives revealed that the oxo−iron bond weakens as

(14) (a) Castellino, A. J.; Bruce, T. C. *J. Am. Chem. Soc.* **1988**, *110*, 158. (b) Lee, Y. J.; Kim, C.; Kim, Y.; Han, S.-Y.; Nam, W. *Bull. Korean Chem. Soc.* **1998**, *19*, 1021.
(15) de Visser, S. P.; Kumar, D.; Shaik, S. *J. Inorg. Biochem.* **2004**, *98*, 1183.
(16) Groves, J. T.; Watanabe, Y. *J. Am. Chem. Soc.* **1986**, *108*, 507.
(17) Studies that focus on the reaction between $TMP^{\bullet+}(Fe^{IV})$═O and *cis*-stilbene to observe similar olefin adduct (viz. $TMP^{\bullet+}(Fe^{IV})$═O-stilbene) formation in CH_3CN are underway in our laboratories.
(18) Collman, J. P.; Kodadek, T.; Raybuck, S. A.; Meunier, B. *Proc. Natl. Acad. Sci. U.S.A.* **1983**, *80*, 7039.
(19) Czarnecki, K.; Nimri, S.; Gross, Z.; Proniewicz, L. M.; Kincaid, J. R. *J. Am. Chem. Soc.* **1996**, *118*, 2929.

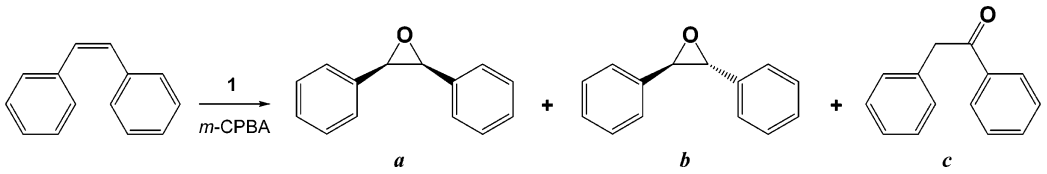

Figure 8. Epoxidation of *cis*-stilbene to form a mixture of *cis*-stilbene epoxide (a), *trans*-stilbene epoxide (b), and deoxybenzoin (c).

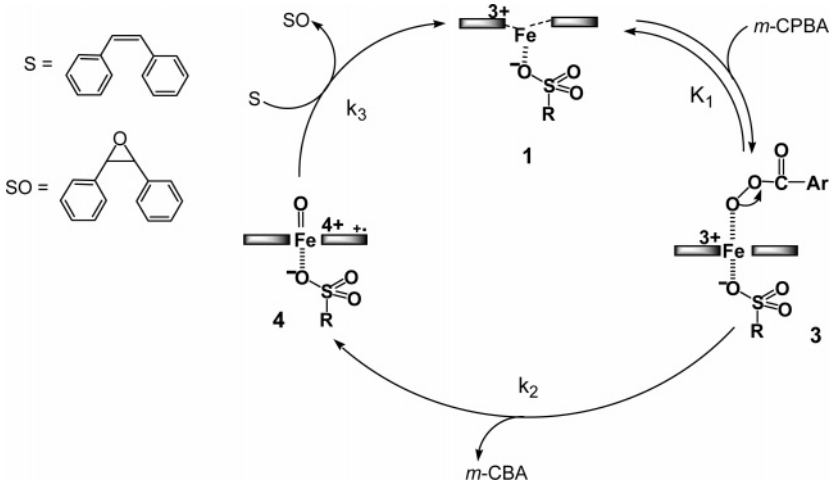

Figure 9. Catalytic cycle for the P450 mimic **1** with *cis*-stilbene in the presence of *m*-CPBA.

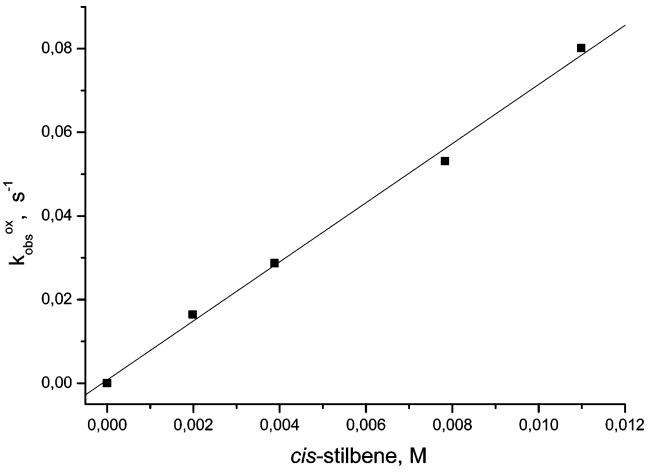

Figure 10. Substrate concentration dependence of k_{obs}^{ox} for the reaction of **4** with *cis*-stilbene. Experimental conditions: [**1**] = 7.9×10^{-6} M, [*m*-CPBA] = 7.9×10^{-5} M, [*cis*-stilbene] = $(1.98-11.0) \times 10^{-3}$ M.

the trans ligand bond strength increases (i.e., CpdI models with stronger binding anions should be more reactive species than their analogues possessing weak donating axial ligands). Recently, Newcomb et al.[20] reported second-order rate constants for the reactions of iron(IV)−oxo porphyrin radical cations generated from either TMP or tetrakispentafluorophenyl iron porphyrin with various substrates, including *cis*-stilbene. Interestingly, the rate constants measured for oxo−iron(IV) porphyrin radical cations depend on the counterion (only a small effect was observed since both selected axial ligands, viz. Cl^- and ClO_4^-, are relatively weak donors) and the solvent, but in general are of the same order of magnitude between 90 and 320 M^{-1} s^{-1} similar to the rate constant of **4** extrapolated to 25 °C, viz. $k_3 = \sim 448$ M^{-1} s^{-1}. These values are so close that any interpretation in terms of structural differences of the porphyrins and axial ligands is useless. Moreover, taking into account that epoxidation reactions consist of two steps (which can be both partially rate-limiting),[16,21] the differences in the reactivity of various model catalysts toward substrate should be accounted for not only in terms of the electronic structure of the CpdI models but also in terms of mechanistic aspects of oxidation reactions such as possible changes in the mechanism and rate-limiting steps.

Discrepancies between rate constants determined for oxygen atom transfer by model ($Por^{\bullet+}$)Fe^{IV}═O species and those observed for the native enzymes[22] point to the important and unique role of the protein architecture in the active heme pocket in modulating the reactivity of the reactive intermediates in the catalytic cycle of P450 enzymes. For example, rate constants for chloroperoxidase CpdI oxidation reactions are 2−3 orders of magnitude larger than those for CpdI models.[20,22b,23] The use of organic aprotic solvents in the study of P450 models can result in stabilization of the intermediates produced in the "peroxy-shunt" reactions, which in turn leads to a decrease in reactivity. In the present study, relatively low rate constants observed for the oxidation reaction of *cis*-stilbene by **4** can also be accounted for in terms of the much higher stabilization of reactive intermediates (in this case **4**) in organic aprotic solvents such as acetonitrile. The apparent rapid reaction observed in Figure 5A on the addition of *cis*-stilbene is still comparatively slow because of the stabilization of **4** by the aprotic solvent used. Work by Mabrouk[24] has clearly demonstrated the possible

(20) Pan, Z.; Zhang, R.; Newcomb, M. *J. Inorg. Biochem.* **2006**, *100*, 524.

(21) (a) Arasasingham, R. D.; He, G.-X.; Bruice, T. C. *J. Am. Chem. Soc.* **1993**, *115*, 7985. (b) Collman, J. P.; Kodadek, T.; Brauman, J. I. *J. Am. Chem. Soc.* **1986**, *108*, 2588. (c) Groves, J. T.; Avaria-Neisser, G. E.; Fish, K. M.; Imachi, M.; Kuczkowski, R. L. *J. Am. Chem. Soc.* **1986**, *108*, 3837.

(22) (a) Watanabe, Y. *J. Biol. Inorg. Chem.* **2001**, *6*, 846. (b) Newcomb, M.; Chandrasena, R. E. P. *Biochem. Biophys. Res. Commun.* **2005**, *338*, 394.

(23) (a) Zhang, R.; Chandrasena, R. E. P.; Martinez, E., II; Horner, J. H.; Newcomb, M. *Org. Lett.* **2005**, *7*, 1193. (b) Zhang, R.; Nagraj, N.; Lansakara-P., D. S. P.; Hager, L. P.; Newcomb, M. *Org. Lett.* **2006**, *8*, 2731.

(24) Mabrouk, P. A. *J. Am. Chem. Soc.* **1995**, *117*, 2141.

benefits of nonaqueous media in facilitating the stabilization of enzyme intermediates in complex biochemical mechanisms.

Conclusions

In summary, we showed in the present study that the new mimic of cytochrome P450 with a substituted RSO_3^- group in organic solvents such as acetonitrile seems to be an effective model system for the study of intermediate states in the reaction cycle of P450. Indeed, with the application of a low-temperature, rapid-scan, stopped-flow technique, we were able to determine equilibrium and rate constants for the formation and decay of intermediates in the catalytic cycle of **1**, including the formation constant of the acylperoxo−iron(III) porphyrin complex (**3**), the first-order rate constant for the heterolytic O−O bond cleavage in **3** (formation of **4**), as well as the second-order rate constant for the oxygen atom transfer from **4** to substrate, a reaction leading to almost complete re-formation of the starting complex **1** (see overall catalytic cycle in Figure 9). We can conclude that complex **1** is a valuable catalyst with promising properties for further applications in a biomimetic approach toward mimicking oxygenation reactions of cytochrome P450. Studies that focus on the determination of activation parameters and elucidation of the detailed mechanisms of oxo−iron(IV) porphyrin π-cation radical formation from complexes **1** and **2** in various organic solvents are currently underway in our laboratories.

Acknowledgment. We gratefully acknowledge financial support from the Deutsche Forschungsgemeinschaft (SPP 1118 and SFB 583) and the Swiss National Science Foundation.

JA073266F